31
Mechanism of Enantioselective Hydrogenation

John M. Brown

31.1
Introduction

The discovery of the first practical catalyst for homogeneous hydrogenation by Wilkinson, Osborn, Jardine and Young in 1965 [1] occurred at around the same time that others, especially Mislow and Horner [2], were demonstrating that chiral trivalent phosphorus compounds were capable of existing as stable, non-interconverting enantiomers. With suitable adaptation of Wilkinson's catalyst, a prostereogenic alkene could be hydrogenated with preferential formation of one enantiomer of the reduced product. The possibility of such enantioselective hydrogenation was recognized by both Horner [3] and Knowles [4], but it was Knowles who won the race to demonstrate the first example in 1968. This led rapidly to a period of seminal discoveries: the application of chelate biphosphine ligands came from Kagan [5], and the development of a full-scale enantioselective hydrogenation of a dehydroamino acid to provide a rhodium-complex-based catalytic synthesis of L-Dopa by Knowles' team at Monsanto [6]. For many years this provided a substantial part of the supply of the main drug active in the control of Parkinson's disease. Kagan was also the first to demonstrate, in his synthesis and application of DIOP (derived very simply from *RR*- or *SS*-tartaric acid), that the difficult synthesis of enantiomerically pure phosphines was unnecessary for effective enantioselective hydrogenation, since a suitable chelate backbone could provide the necessary level of stereochemical control. For many years the development of enantioselective hydrogenation converged on the preparation of enantiomerically pure chelate diphosphines and the application of their rhodium complexes to the hydrogenation of dehydroamino acids, enamides and closely related reactants [7]. Although both ruthenium [8] and iridium catalysts [9] for homogeneous hydrogenation were known at an early stage, the development of effective enantioselective hydrogenation in these two spheres occurred much later. For ruthenium enantioselective hydrogenation, the spectacular efficiency of BINAP catalysts [10] developed by Noyori's group was first demonstrated for alkenes, and then in rather greater depth for ketones [11]. The high efficiency of iridium complexes in hydrogenation had been demonstrated

The Handbook of Homogeneous Hydrogenation.
Edited by J.G. de Vries and C.J. Elsevier

ISBN: 978-3-527-31161-3

in **1976** by Crabtree and Morris [9], but it was 20 years later before Pfaltz and Lightfoot developed the first asymmetric variant [12]. Whilst initially rather slow to recognize the potential of asymmetric hydrogenation, and enantioselective catalysis in general for industrial scale-up, the pharmaceutical and fine chemical industries are in the forefront of current developments [13]. The ease of operation of homogeneous catalytic hydrogenation, the high stereochemical efficiency and the wide range of reactants which are currently amenable to the procedures make this a versatile synthetic method at all scales.

31.2 Rhodium-Catalyzed Hydrogenations

31.2.1 Background

The mechanism of enantioselective hydrogenation by rhodium complexes has been reviewed on several occasions, including a recent detailed publication by the present author [14]. In addition, much of the contemporary work by Gridnev and Imamoto has been reviewed, as described below. Consequently, details of the older studies will be cited only briefly to provide the necessary context, after which the post-1998 developments will be discussed in detail. For a mature field, it is surprising how much new and significant information has been reported during the past five years.

Older studies into the mechanism of enantioselective hydrogenation were characterized by two main approaches: (i) the measurement and detailed analysis of reaction kinetics by Halpern and coworkers [15]; and (ii) the characterization of reactive intermediates in solution by NMR [16], augmented by X-ray analyses and other physico-chemical techniques. The rhodium catalyst is frequently introduced as a cationic diphosphine dialkene complex which requires an initial hydrogenation of the dialkene before an active catalyst is formed. Heller and coworkers have studied this process in some depth [17]. Hydrogenation of the first double bond *in situ* may be followed by a sequential hydrogenation of the now freely dissociating mono-alkene. With a high [Rh]/[substrate] ratio (typical of small-scale work), precatalyst reduction can influence the rate of hydrogenation of the substrate, and the reactivity of norbornadiene and cycloocta-1,5-diene precatalysts is distinct. Overall, the accumulated mechanistic evidence indicates several key features of the reaction mechanism, which made it distinct from the simple Wilkinson's hydrogenation pathway:

- In the absence of reactant, (cationic) biphosphine rhodium complexes exist in methanol, the generally preferred reaction medium, as a *bis*-solvate. The affinity for dihydrogen is low.
- In the presence of the dehydroamino acid reactant, bidentate complexation as an enamide occurs. With a chiral diphosphine ligand, two diastereomeric forms of the enamide complex are observed in equilibrium that differ in the

prostereogenic face of the alkene bound to rhodium. The major species in solution corresponds with the isomer characterized by X-ray crystallography. The association constant for enamide formation varies widely with the ligand, with smaller bite angles tending to give stronger binding.

- At low temperatures, only the disfavored enamide complex reacts with dihydrogen, forming an alkylhydride complex that decomposes to form the hydrogenation product above –50 °C. No evidence for an intermediate dihydride could be established, although its involvement was assumed. All of the described intermediates give well-defined and distinctive NMR spectra in which ^{1}H, ^{31}P and ^{13}C (with enrichment) are all informative.
- Dihydrogen addition to the enamide complex is rate-limiting and irreversible. With *para*-enriched hydrogen, there is no *ortho-para* equilibration in a dehydroamino acid turnover system until hydrogenation is complete [18] (this last precept has come under recent close scrutiny).

These observations and results can be expressed in the "hour-glass" double catalytic cycle first briefly introduced by Brown and coworkers [19], but indelibly associated with the detailed kinetic study of Clark and Landis (Fig. 31.1) [15 a]. For this study, the Monsanto ligand DIPAMP was selected and this proved to be especially revealing. Because the enamide complexes are formed here with a particularly strong association complex, the enantiomer excess in hydrogenation is very sensitive to the temperature and dihydrogen pressure. Access to the "minor enamide" pathway is controlled by the depth of the ground-state energy-well associated with the major enamide complex. This influences the extent to which the minor enamide pathway dominates catalysis, and permits the direct testing of the model over a wide range of conditions, with excellent correlation between experiment and theory.

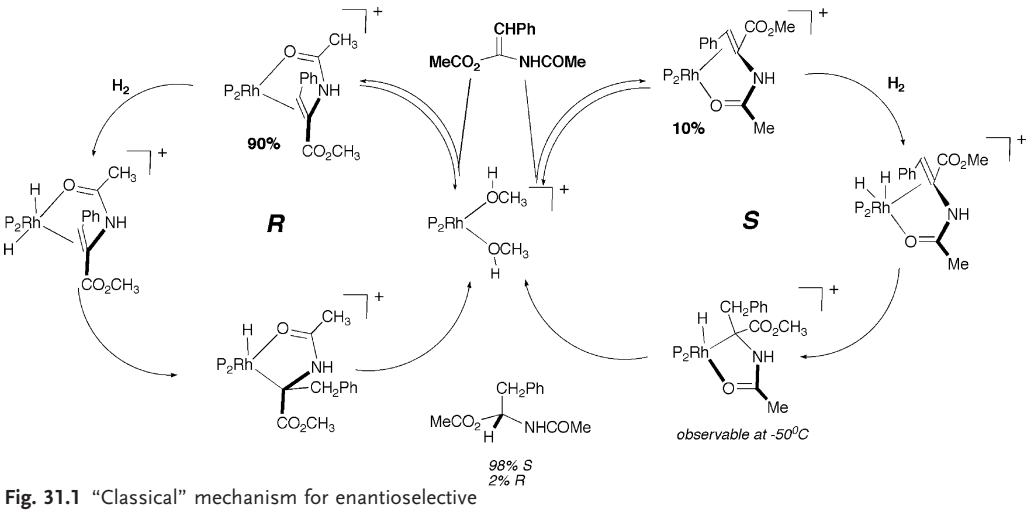

Fig. 31.1 "Classical" mechanism for enantioselective hydrogenation [15a,b, 19]; P_2 = (*R*,*R*)-DIPAMP.

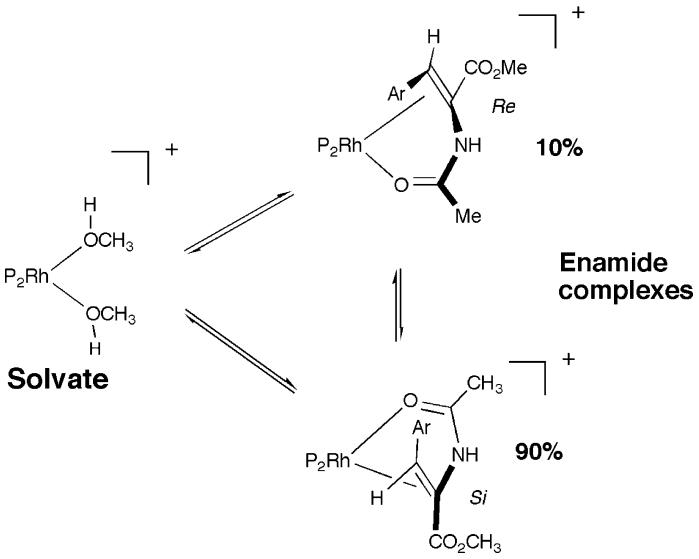

Fig. 31.2 Typically (DIPAMP, CHIRAPHOS), the intramolecular exchange of *Re* and *Si* complexes is several times faster than the dissociation to reform the solvate complex.

In this kinetic study, the interconversion of the two diastereomeric enamide complexes was treated as a dissociative process, proceeding through the solvate complex. This is not the main pathway, as clearly revealed by spin-saturation ^{31}P-NMR experiments that demonstrate the retention of identity of the two separate phosphorus nuclei during the exchange process; a solvate has equivalent ^{31}P sites [20]. The recognition that this intramolecular process is occurring requires some modification of the rate constants, but not the fundamental mechanistic principles enshrined in the model. It is a general and fundamentally important fact that the processes of Figure 31.2 are fast relative to catalytic turnover.

31.2.2
More Recent Developments

Mechanistic studies carried out up to the late 1990s served to reinforce rather than to overturn the mechanistic models then in place. During that period there had also been significant developments in ligand design that greatly enhanced the utility and range of rhodium enantioselective hydrogenation. The first major contribution came from Dupont, where Burk and coworkers synthesized the DUPHOS ligand family and showed how their rhodium complexes were significantly superior to any previous examples, and made enantioselective hydrogenation a far more general synthetic reaction [21]. A key factor was the phospholane structure; part of the culture of the subject had been built around the idea that arylphosphine

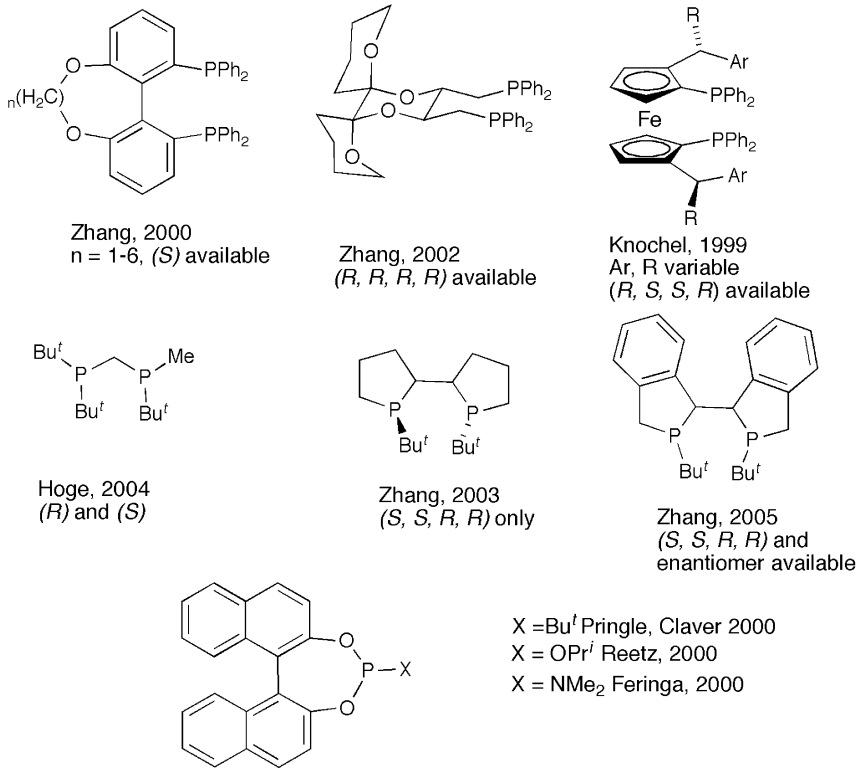

Fig. 31.3 Examples of second- and third-generation phosphine and diphosphine ligands.

moieties played a crucial part in enantioselection. With alkylphosphines now also seen to be important, Evans and coworkers demonstrated a neat synthesis of enantiomerically enriched variants by the sparteine-promoted deprotonation of one of the diastereotopic methyl groups of $H_3B \cdot PBu^t(CH_3)_2$ [22]. This discovery enabled Imamoto's group to synthesize a range of diphosphines based on the general motif $R_LR_SP(X)PR_SR_L$, where R_S and R_L are small and large alkyl groups respectively and (X) represents the chelate backbone [23]. Other notable successes have been obtained with electron-rich diphosphines such as the PHANEPHOS ligand based on [2.2]-paracyclophane [24]. The design of effective electron-rich ligands for enantioselective catalysis based on these and related themes, has been a trademark of Zhang's studies [25]. In parallel with these developments of new families of chelate diphosphines, new investigations – most effectively developed by Feringa's group after three near-concurrent reports [26] – have demonstrated the comparable utility of appropriately designed monophosphines or other P(III) compounds (Fig. 31.3). In considering the practical applications of a particular ligand, it is important to determine whether the required enantiomer is easily available. In several cases, especially where phosphorus chirality is involved, only one of the two may be accessed readily.

The enhanced synthetic potential of rhodium-complex-catalyzed enantioselective hydrogenation provided by these advances in ligand design has led to renewed interest in the reaction mechanism, and here we highlight four recent topics: (i) the extended base of reactive intermediates; (ii) an improved quadrant model for ligand–substrate interactions; (iii) computational approaches to mechanism; and (iv) (*bis*)-monophosphine rhodium complexes in enantioselective hydrogenation. These are discussed in turn.

31.2.3
Transient and Reactive Intermediates in Rhodium Enantioselective Hydrogenation

The status quo provided by the early mechanistic studies described above was incomplete in several respects. Although the affinity of the solvate complex for dihydrogen was known to be low, the addition product remained uncharacterized. Likewise, the putative H_2 addition intermediate between the enamide complex and the transient, but observable, alkylhydride had not been characterized.

A common characteristic of the "second generation" of ligands for enantioselective hydrogenation is the electron-rich nature of the diphosphine. The electronic character of the ligand will of course affect the relative stability of different states in the catalytic cycle and influence their accessibility. In the "classical" biarylphosphine-based chemistry, formation of a stable dihydride from the initial 16-electron Rh solvate complex had never been demonstrated. The fleeting existence of a hydridic intermediate could be inferred from the reversible *ortho-para* equilibration of dihydrogen by the solvate complex [17]. In a thorough study of observable intermediates in the catalytic cycle of dehydroamino acid hydrogenation by the C_2-symmetric ligand BisP* (see Fig. 31.4), a solvate dihydride was characterized for the first time at low temperatures [27]. The complex, present to the extent of ca. 20% at –90 °C under ambient hydrogen pressure, existed as an unequal pair of rapidly equilibrating diastereoisomers. When hydrogen deuteride (HD) was employed, the D-*trans*-solvent isomers predominated by 1.3 : 1. The derived equilibrium constant at 20 °C implies that the dihydride is present to only a minor extent at $[H_2] = 4$ mM, the ambient equilibrium concentration. Within the same family of alkylphosphine chelates, the larger bite angle of the xylylene-bridged complex permits the exclusive formation of a pair of diastereomeric solvate dihydrides at –70 °C, persistent to –20 °C [28]. With the lower homologue of the bis-P* ligand (Miniphos), the isolated complexes tend to be of the general structure $(P_2)_2Rh^+$. Reaction with dihydrogen provides NMR-characterizable complexes of the form $(P_2)_2RhH_2^+$, and hydrogenation can proceed from this state by complete dissociation of one diphosphine moiety [29]. At ambient temperature this is transformed into a bridged dihydride complex. A further example of a stable solvate dihydride was obtained during a study of the reaction of PHANEPHOS rhodium complexes with *para*-enriched dihydrogen. In the presence of a dehydroamino ester, a diastereomeric pair of spin-excited solvate dihydride complexes could be identified, structurally related to the examples described above [30].

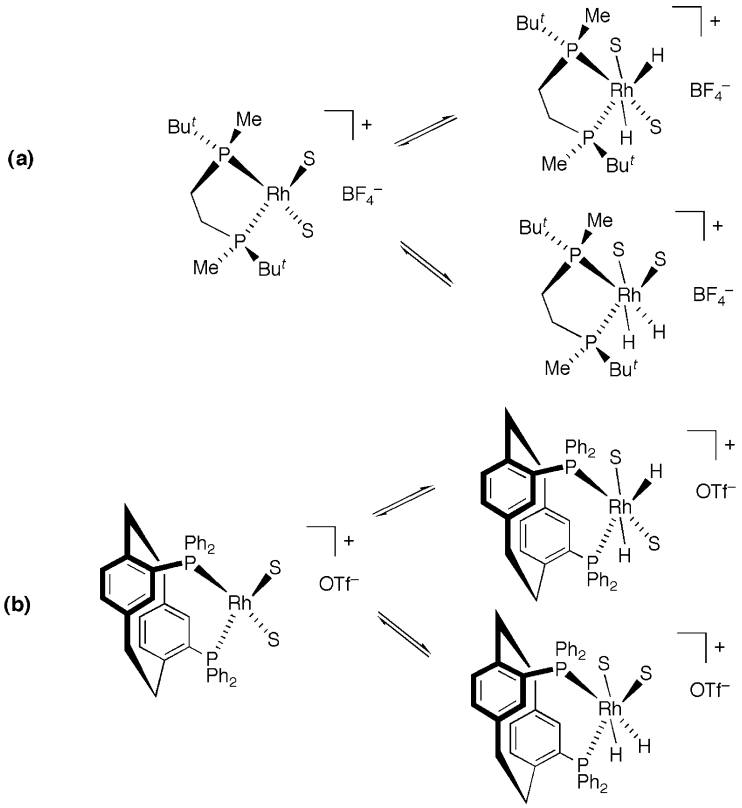

Fig. 31.4 Solvate dihydrides characterized at low temperature [S=CH_3OH or CD_3OD]. Dihydrides formed *in situ* react rapidly with the common substrates of enantioselective hydrogenation, and the reduced product is formed with high enantioselectivity. At ambient pressure, the proportion of dihydrides is 45% at –100 °C for (a) with a 10:1 diastereomer ratio, and 40% for (b) at –40 °C, with a 2:1 diastereomer ratio.

The accepted mechanism for hydrogenation of alkenes by Wilkinson's catalyst involves the addition of dihydrogen prior to coordination of the alkene, followed by migratory insertion [31]. The new demonstrations of the existence of solvate dihydride complexes inevitably raise the question as to whether the same mechanism can apply in rhodium enantioselective hydrogenation. The evidence in support of this possibility is analyzed in more detail later.

Whatever the route to a rhodium dihydride alkene complex, the hydrogen must be transferred sequentially to the double bond. It had always been assumed that the first C–H bond is formed β to the amido-group, so that the more stable Rh–substrate chelate is formed. This is the alkylhydride isomer observed in stoichiometric NMR studies at low temperatures, and is supported by studies under catalytic turnover conditions, assuming a normal isotope effect.

Thus, earlier studies by Brown and Parker [32] had shown that the isotope partitioning in catalyzed HD addition to dehydroamino esters indicated predominant prior migration of H to the β-position of the ensuing amino acid derivative so that the α-position was relatively rich in D. This sequence is not invariably observed, however. A key experiment was based on a prior observation by Burk's group that the stereochemical course of enantioselective hydrogenation of two closely related enamides was diametrically opposite [33]. In order to confirm that a fundamental change in mechanism is responsible, an HD isotope partitioning experiment was carried out for these substrates (Fig. 31.5) [34]. In this investigation, the pattern of D-substitution was as expected in the product derived from the Ph-substituted enamide, but it was reversed for the Bu^t-substituted enamide. Only the Bu^t-compound gave informative results in NMR studies; the intermediate alkylhydride indicated alkene-only coordination with a non-participating amide, in consequence of the steric bulk of the Bu^t-group. It was assumed that the alkylhydride complex was formed directly from the solvate dihydride and alkene. In examining the same problem, a computational study of the difference between enamides with bulky (Bu^t) and small (CN) substituents predicted opposite product configurations, although chelated substrates were employed in the computational model which contrast with the experimental NMR evidence described above [35].

The enamide dihydride intermediate that precedes migratory insertion has proved elusive, despite one earlier claim where the evidence is incomplete and possibly not correctly interpreted [36]. Hydrogenation by rhodium complexes of

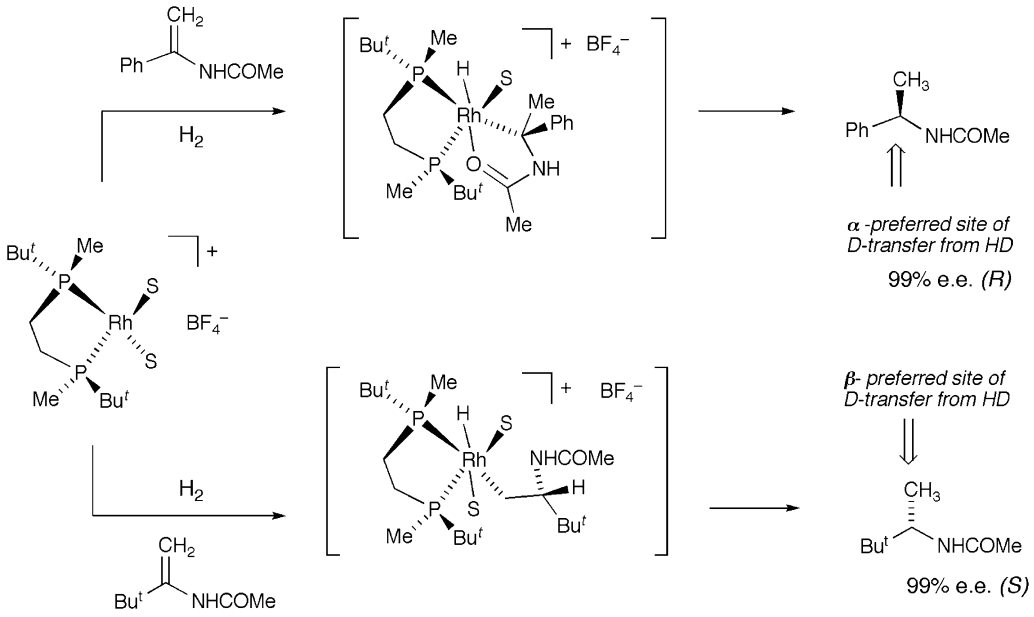

Fig. 31.5 Normal and anomalous pathways for the hydrogenation of alkylenamides.

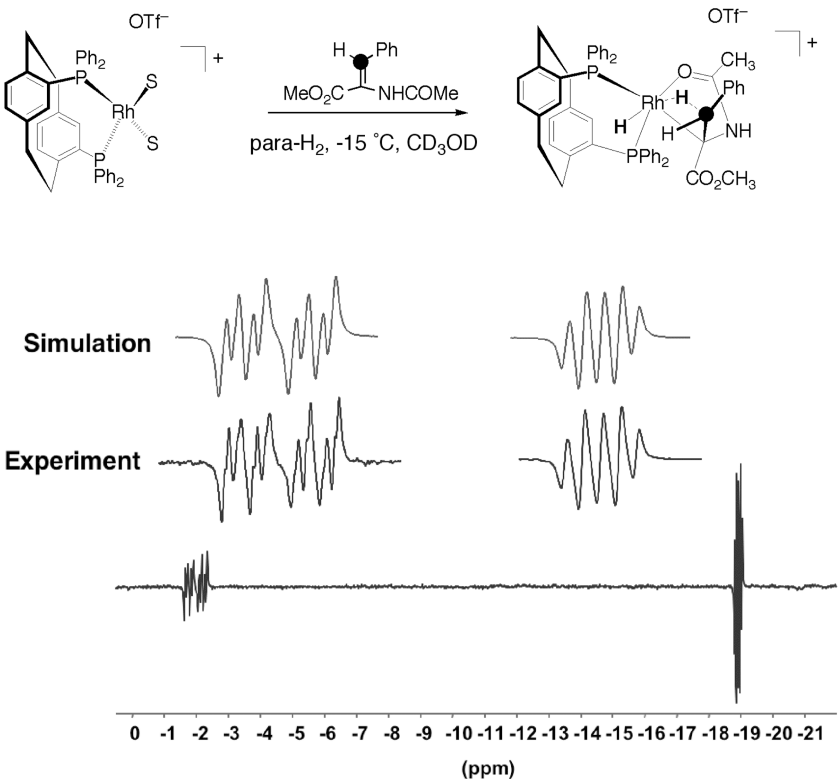

Fig. 31.6 ^{1}H-NMR spectrum of the initial reaction product of β-^{13}C-labeled enamide with *para*-enriched H_2 at –15 °C in CD_3OD; the agostic C–H is at –2 ppm.

the ligand PHANEPHOS occurs under quite unusual conditions (H_2 bubbling through substrate solution at –40 °C), and is applicable to some otherwise sluggish reactions [23]. This suggests a highly reactive catalyst, which could reveal the structure of pre-insertion intermediates. When dehydroamino acid hydrogenation was carried out with *para*-enriched H_2, and the ^{1}H-PHIP-NMR monitored, a new transient dihydride was observed with intact substrate [37] (Fig. 31.6). The transient possessed unusual chemical shifts, and full analysis showed that it was indeed the desired dihydride, but one where a single hydrogen has been captured in agostic flight from rhodium to carbon. Tracking the process of spin excitation indicates that this transient is linked to the hydrogenation product and the $P_2RhS_2^+$ solvate, but not to the reactant. An intrinsic advantage of the PHIP procedure is that the characteristic absorption-emission (AE) spectra are only observed whilst there is spin coupling of the hydrogens of the original *para*-H_2 molecule so that artifacts remain invisible. This is the only example of a dihydride intermediate on the pathway, and may be a special case that demonstrates the unusual properties of this particular ligand.

31.2.4
Mnemonics for the Sense of Enantioselective Hydrogenation

Very early on in the development of enantioselective hydrogenation it was recognized that a simple rule that linked the stereochemical course of the reaction to the structure of the ligand would be exceedingly valuable. Several efforts were made in this direction: Kagan linked the chelate twist (λ or δ) to the predominant enantiomer [38], while Kyba considered the sense of twist of the dialkene precursor of the catalyst [39] and Knowles introduced the Quadrant Rule [40]. The last of these was potentially more useful than the others, since it specifically considered the binding of substrate. The C_2-symmetrical ligand was considered as $R_LR_SP(X)PR_SR_L$ with the bulky R_L ligands disposed to equatorial positions in the chelate ring and R_S to axial positions. That was consistent with X-ray crystallographic evidence available at the time, which also indicated that in a square-planar complex the equatorial groups have closer contact to the bound substrate than the axial groups. The rule was incomplete in its predictive power in its original form, however, and needed correction. With the advent of a new generation of electron-rich alkylphosphine ligands it was first realized in a report by Marinetti and coworkers that even Knowle's modified Quadrant Rule failed

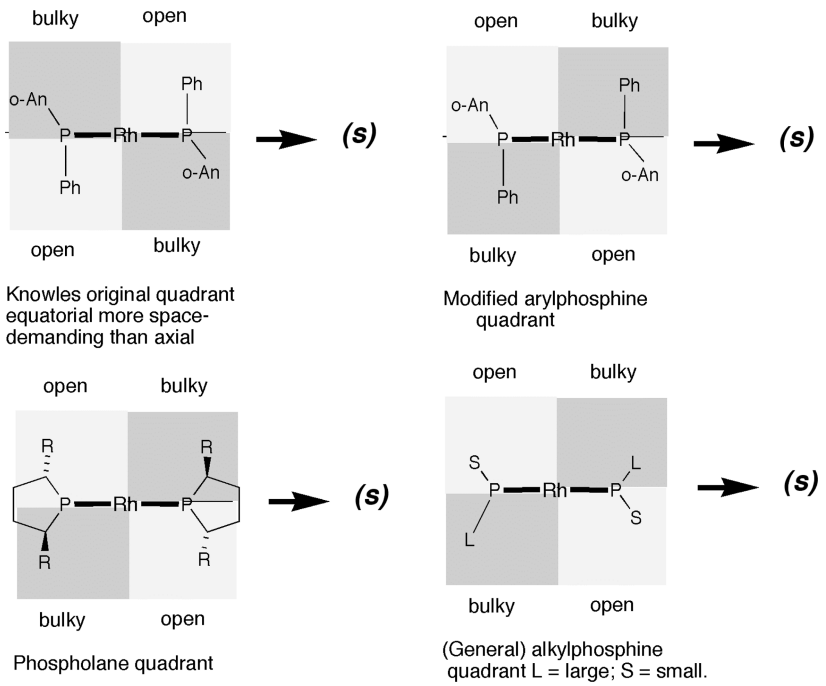

Fig. 31.7 Modern presentations of the Quadrant Rule for predicting the course of enamide hydrogenation, following the original work of Knowles.

to make the correct predictions [41]. The reasons for this become clear when the basis of the rule is considered; it analyzes the steric interactions that exist in a four-coordinate square-planar intermediate. It remained for Gridnev and Imamoto to reassess the analysis and present an alternative that may have far more general applicability [42]. In their modified model, the important stereodetermining step is six-coordinate and located at the point where both dihydrogen and the chelating reactant are bound. With this modification, the bulky groups in a diarylphosphine chelate are defined as the axial rather than the equatorial phenyls, the opposite of the original indications of Knowles. The current status of the Quadrant Rule and its relationship to the original form, now applicable to a much broader range of ligands, is shown in Figure 31.7. Formulation of this Rule in specific cases is aided by a thorough analysis of the X-ray structures of the "precatalyst" diolefin complex, with respect to the bite angle and coordination geometry of the dialkene [43].

31.2.5
Status of the Computational Study of Rhodium-Complex-Catalyzed Enantioselective Hydrogenation

The development of density function theory (DFT), together with the rapid increase in computational power experienced during the last decade, has made real homogeneous catalytic systems accessible to quantum mechanical calculations. In the study of enantioselective hydrogenation, one sequence of investigations stands out, however. The studies of Feldgus and Landis address the "classical" model of enantioselective hydrogenation without considering more recent investigations into solvate dihydride pathways, but consider the possible routes for that in a high degree of detail [44]. Their first report is concerned with achiral models (Fig. 31.8). Starting with the square-planar enamide complex, the computational analysis centers on the successive formation of a dihydrogen complex, dihydride, alkylhydride and reduced but coordinated product, as well as the intervening transition states. At each stage there are several geometrical isomers to be considered, and the computational process treats the intermediate species as non-interconverting, save for the dihydride. Although the computation was carried out with $(PH_3)_2$ as model ligand, only species with *cis*-phosphine geometry were considered. With these constraints, the energy surface was constructed for four possible pathways defined by the four possible approach trajectories of H_2 towards the square-planar enamide complex (above and below the two linear axes), each of which flows through a sequence of distinct geometrical isomers. The interconversion of isomers at the dihydride level was analyzed independently by an alkene dissociation pathway, the only one that was energetically viable. These results demonstrate the feasibility of interconversion with a computed barrier of 14.1 kcal mol^{-1}. The kinetic isotope effects for the steps affected by isotope substitution and the consequences of reduction of the substrate by HD are also studied. When addition of $H_2(D_2)$ is turnover-limiting, a significant isotope effect should be observed (1.4–1.7). For the case that insertion is turnover-

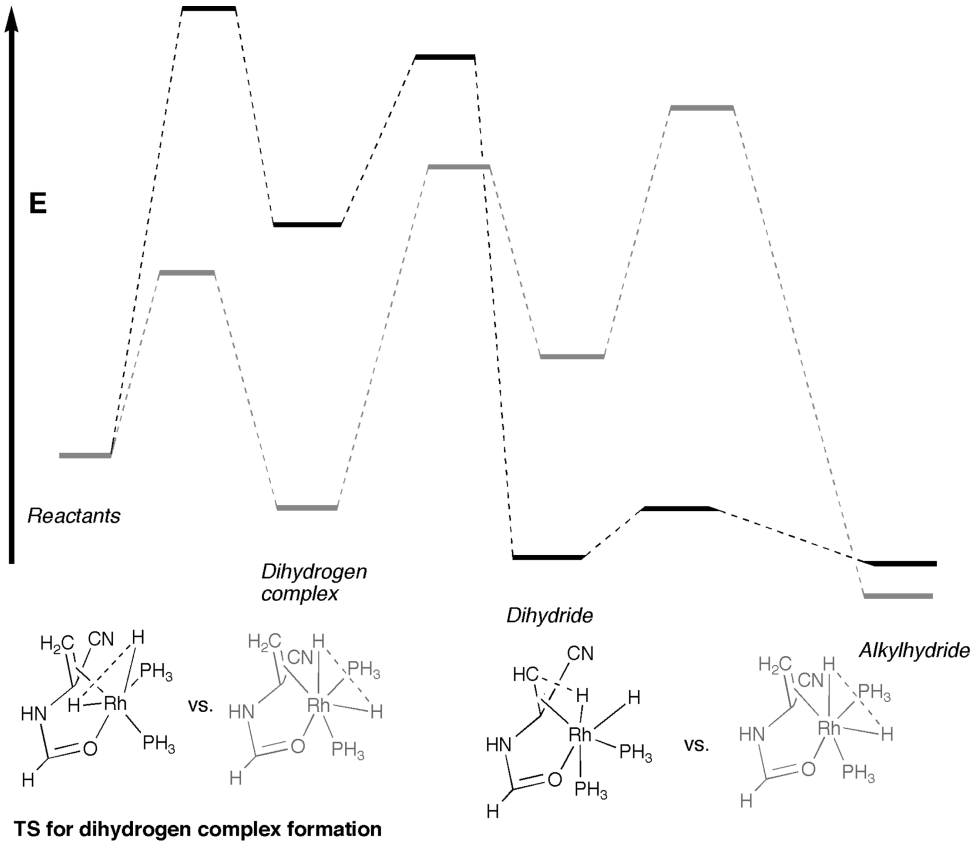

Fig. 31.8 Two of the four possible pathways in the hydrogenation of the model complex shown; schematic energies derived from DFT calculations. The alternative routes are associated with higher barriers. The absolute energies, but not the main conclusions, are unaltered when $2\times PH_3$ is replaced by $Me_2P(CH_2)_2PMe_2$.

limiting, the kinetic isotope effect is small and in keeping with experimental results (1.0–1.15). The experimental result for HD addition to the dehydroamino ester places the D-atom predominantly at the α-position of the reduced product. This is replicated only by the turnover-limiting insertion mechanism, and not the alternative oxidative addition. The conclusions of course assume comparability between the simple model phosphines and the "real" ligand.

The success in a simple model system encouraged Feldgus and Landis to study the fuller DUPHOS-based system for enantioselective hydrogenation (as defined in Fig. 31.9) [45]. ONIOM methods were required because of the level of complexity; a core of the rhodium-complexed atoms was treated by DFT at B3LYP level, the core organic atoms at Hartree-Fock level, and the remainder by

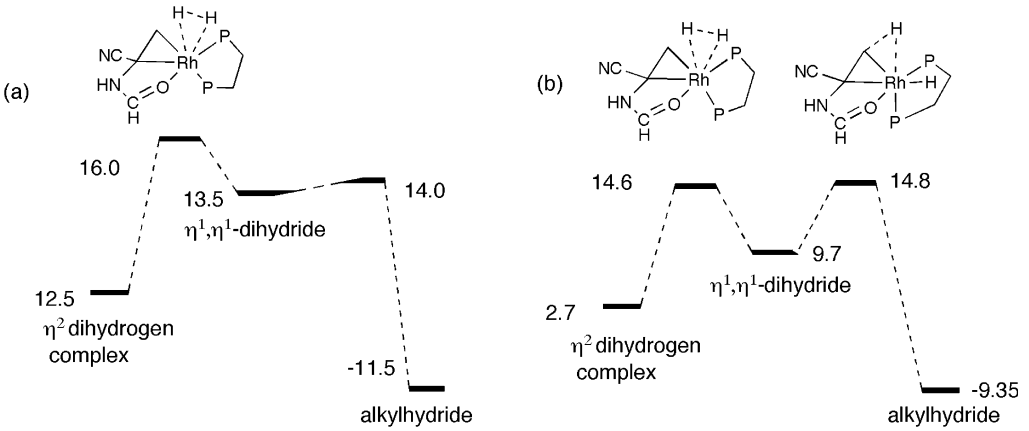

Fig. 31.9 Turnover-limiting transition states for enantioselective hydrogenation derived from DFT calculations. (a) ONIOM calculations, PP = Me-DUPHOS [45]. (b) Full computation on all atoms, PP = *bis*-PP* with a rigid Et group to simulate Bu^t [47]. Numbers refer to the energy in kcal mol^{-1} of the states relative to the resting state.

molecular mechanics (MM), employing Landis' universal force field (UFF) method. The same steps were carried out in the computation as before, but now two diastereoisomeric pathways can be considered. It was assumed that the two possible enamide complexes do not interconvert other than through the solvate, at variance with experimental observation [46], and that there is no other crossover possible between the two pathways. Nevertheless, the computation correctly predicts the difference in ground-state energy favoring the major diastereomer of enamide complex, and the lower energy pathway for hydrogenation that is available to the minor diastereomer. Of the four stereochemically distinct pathways considered in the earlier report, the same one (Feldgus and Landis' path **A**) is found to be most favorable here. The most interesting difference found in the full model is that H_2 addition rather than migratory insertion is turnover-limiting. These observations inspire confidence that the transition-state structures being considered in the turnover-limiting region make accurate predictions about the outcome of asymmetric hydrogenation. Much still remains to be considered and evaluated at a level of detail.

In a later approach, using B3LYP, DFT with the same basis sets as above was applied to all atom computation for the pathway in enantioselective hydrogenation by bisP*Rh^+. At this higher level of theory, the turnover-limiting transition state was at a similar position on the energy profile for both diastereomeric pathways [47]. This involved the early part of the H_2 addition to form an η^2-complex, which then goes on to form the dihydride, but by (reversibly) traversing a low energy barrier. The two transition states relevant to limiting turnover here are the initial H_2 addition and the conversion of the η^2-dihydrogen complex into a η^1,η^1-dihydride; the second of these is very slightly higher in energy

than the first. The same conclusions as before were drawn concerning the energetic preference for reaction via the minor diastereomer, and by a clear margin. The general comment needs to be made that increasing computer power, and increasing sophistication of the theoretical model, will lead to alteration of the detailed energy surface for enantioselective hydrogenation without altering the fundamental conclusions.

31.2.6 Monophosphines in Rhodium-Complex-Catalyzed Enantioselective Hydrogenation

A significant success was achieved by Knowles and his colleagues using the monophosphine CAMP, describing work that paved the way to practical applications of asymmetric hydrogenation [48]. Largely because of difficulties in obtaining the ligand enantiomerically pure, attention soon switched to C_2-symmetrical diphosphines (DIPAMP, DIOP) where the problem was averted or controlled. It has only been during the past few years that monoligating phosphanes have reasserted prominence (Fig. 31.10). An initial report by Guillen and Fiaud on the efficacy of monophospholanes [49] was rapidly followed by several further reports [25]. Among these, the studies of Feringa, de Vries and colleagues on BINOL-derived phosphoramidites have been developed most vigorously [50]. The observed reactivity of phosphoramidites as ligands in the Rh-catalyzed hydrogenation of both α- and β-dehydroaminoacids is comparable to that of the commonly employed diphosphines [51]. It is very likely that two molecules of the monophosphane are involved in coordination to rhodium throughout the catalytic cycle. There is a pronounced positive non-linear effect when scalemic phosphoramidite is employed. Solutions containing less than 2 equiv. of the monodentate ligand per rhodium provide for reactive catalysis. There is a rate dependence on the L/Rh ratio, but the *ee* remains constant over the L/Rh range of 1 to 2. This result was attributed to the tendency of *bis*(monophosphane)-rhodium complexes to disproportionate, unlike their diphosphane-rhodium analogues. Electrospray-mass spectrometry (ES-MS) analysis of the reacting solution revealed the presence of P_1Rh^+, P_2Rh^+, P_3Rh^+ and P_4Rh^+ at different times, and also that the initial $[P_2Rh(norbornadiene)]^+$ complex persists for long periods after the initiation of hydrogenation [52]. With two different phosphorus ligands in combination, the *ee* in hydrogenation may be enhanced over their separate use, indicating that the catalytic intermediate leading to enantiodifferentiation incorporates both ligands. This is reinforced by the observation that a combination of enantiopure and achiral ligands leads to different results from the enantiopure ligand alone; in some cases the incorporation of the achiral partner leads to reversal of the sense of enantioselectivity. Excellent results may be obtained in the rhodium-complex-catalyzed hydrogenation of a simple dehydroamino ester with a 1:1 mixture of an atropisomerically stable BINOL-derived phosphite and a related configurationally labile 2,2′-biphenol-derived phosphite. It proved difficult to put these observations on a more quantitative footing because the catalyst system is complex under turnover conditions [53].

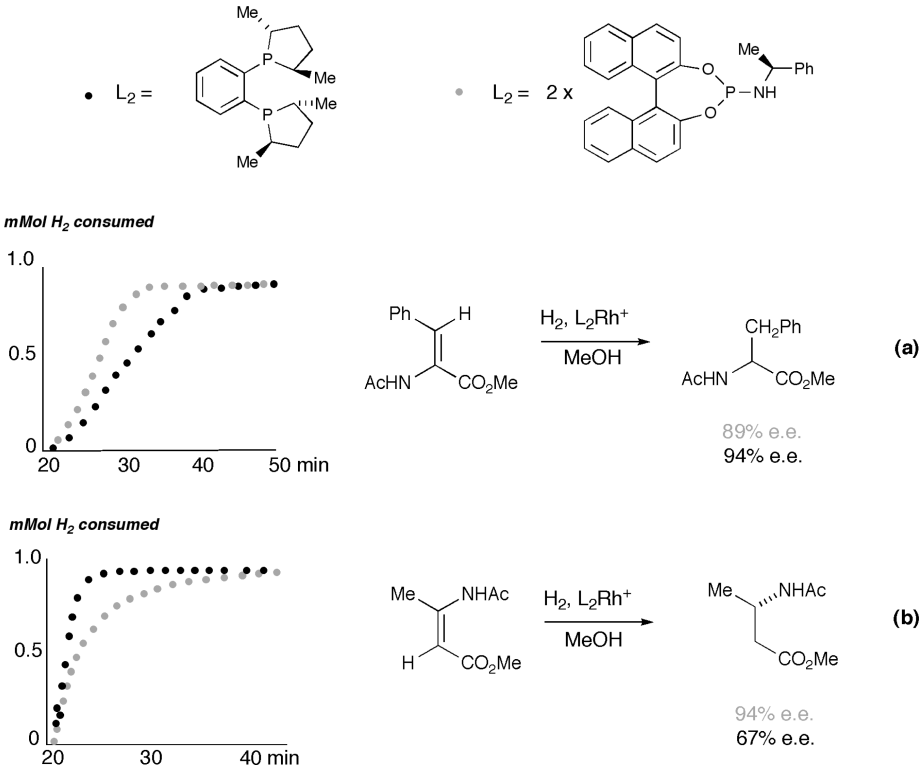

Fig. 31.10 Comparison of rate (schematic) and enantioselectivity for mono- and bidentate phosphorus ligands on 1 mM scale. (a) α-Dehydroamino ester, 2 bar H_2; (b) β-dehydroamino ester, 10 bar H_2.

31.2.7
Mechanism of Hydrogenation of β-Dehydroamino Acid Precursors

As the range of rhodium enantioselective hydrogenation has been extended, new types of reactant have been involved in reduction, and with high enantioselectivity. The synthesis of β-amino acids falls within this compass, and recent examples have demonstrated successful hydrogenation of both (*E*)- and (*Z*)-precursors [54]. This raises the question as to whether the mechanism is the same as has been defined in the α-dehydroamino acid case. The reduction of simple reactants indicated a dramatic difference between the diastereomers, which is part of a generally observed pattern; the (*E*)-isomer gave the better *ee*-values, but only the (*Z*)-isomer showed substantial diminution of enantioselectivity at higher pressures [55]. There is a difference in the enamide association constant from the two reactant diastereomers, with the (*Z*)-isomer the more strongly bound. This can lead to zero-order kinetics for its hydrogenation using DIPAMPRh$^+$, whereas the corresponding (*E*)-isomer hydrogenates with first-order kinetics and

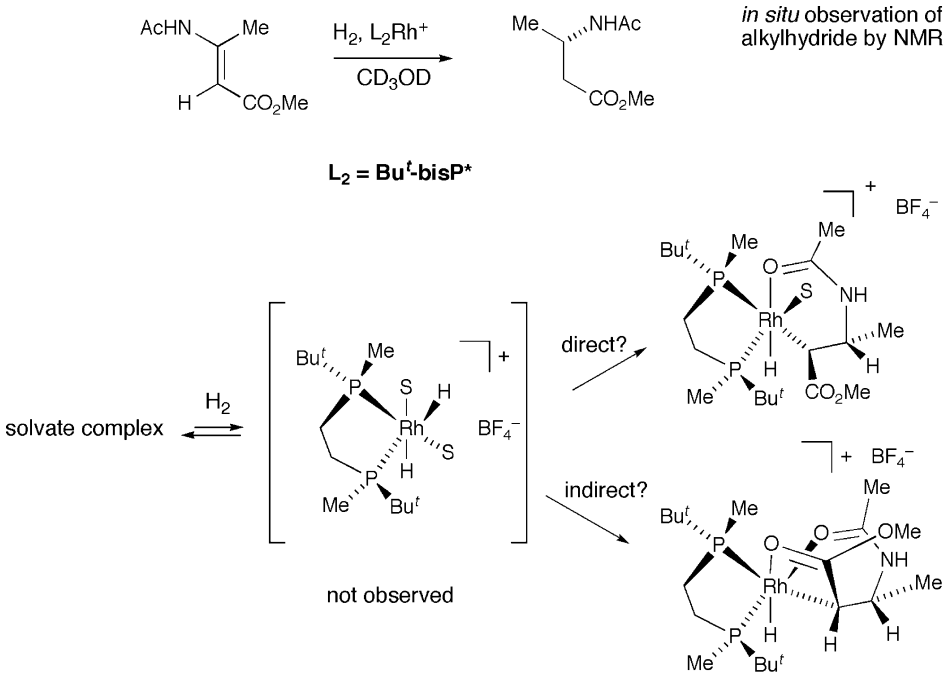

Fig. 31.11 Intermediates in the enantioselective hydrogenation of β-amino ester precursors.

higher *ee*. The accessibility of stable intermediates in this chemistry has led to a different correlation between the configuration of the enamide complexes and the reaction course than for the α-dehydroamino ester case. For two examples, the configuration of the enamide complex established by X-ray corresponds with that of the main hydrogenation product. The authors conclude that there are only slight differences between the hydrogenation activities of the *re*- and *si*-bound diastereomers [56]. *In-situ* study of the intermediates in the hydrogenation of β-dehydroamino esters reveals the formation of several alkylhydrides at low temperatures from the (*E*)-isomer, although only one enantiomer of reduced product is formed [57]. Because the carboxyl group better stabilizes the β-C–Rh bond, the intermediates are formed by hydride delivery to the enamide-bearing carbon, in contrast to the normal α-dehydroamino ester case. This partly explains the absence of the anticipated correlation between enamide configuration and the stereochemical outcome of hydrogenation (Fig. 31.11).

31.2.8
Current Status of Rhodium Hydrogenations

Although the main features of the mechanism have been in place for almost 20 years, recent results have provided considerable refinement. It is becoming clear that a single pathway cannot fit all ligands and all reactants, although there are

common principles, which apply quite generally. Even the paradigm that the configuration of the product is stereochemically related to the less-favored form of the complexed substrate is violable. Evans and coworkers investigated the synthesis and catalytic reactivity of a series of easily prepared P–S chelate ligands in enantioselective catalysis [58]. For hydrogenation, high enantioselectivity was observed in dehydroamino acid reduction (Fig. 31.12). Most significantly, an X-ray structure of the derived enamide complex (shown to be the exclusive diastereomer in solution by NMR) indicated that the alkene was bound to rhodium through the face to which H_2 is delivered during hydrogenation. This of course undermines any absolute rule linking the minor diastereomer with the stereochemical outcome of enantioselective hydrogenation. It does not, however, violate the new statement of the Quadrant Rule, where the geometry of the turnover-limiting reaction transition state is cryptically taken into consideration, so that the correct steric interactions between ligand and bound substrate are properly considered.

The combination of recent studies on reactive intermediates and computation provides a more incisive insight into the reaction mechanism. In particular, the role of the solvate dihydride, now characterized, needs to be readdressed, as does the older idea that dihydrogen addition rather than migratory insertion is the turnover-limiting step. The first of these points needs to be analyzed in terms of known, and accepted, kinetic models. By deriving the formal rate equation, Heller has demonstrated that a catalytic cycle based solely on the initial formation of a solvate dihydride would not show any pressure dependence of *ee* [59]. This is at variance with the original studies of Halpern and Landis, among others. From the careful studies of Imamoto and Gridnev, there is no doubt that the observed solvate dihydride (SH_2) complex reacts rapidly and quantitatively at low temperature with the alkene substrate, giving product with the expected enantioselectivity. Even at the lowest temperatures, SH_2 is only a minor component of the equilibrium mixture. Based on the published equation for the equilibrium thermodynamics, there is substantially less than 0.1% of the dihydride complex present in equilibrium with the solvate complex under ambient conditions. The alkene normally binds strongly to the solvate, displacing the equilibrium and further attenuating the possibility of reaction through that pathway. (In unpublished calculations based on measured equilibrium constants in the DIPHOS-Rh^+-catalyzed hydrogenation of (*Z*)-*α*-methyl acetamidocinnamate and Halpern's kinetic data, an unrealistically high rate constant for the reaction between $Rh(dppe)(MeOH)_2$ and H_2 is required to accommodate the dihydride route; U. Sharma, P.J. Guiry and J.M. Brown, unpublished results.) The observation of SH_2 complexes is in any event limited to the highly electron-rich ligand families synthesized recently. Several of these ligands have shown exceptional promise in the enantioselective hydrogenation of tetrasubstituted alkenes, specifically *β,β*-disubstituted dehydroamino acids [60]. These are precisely the cases where reactant binding to the solvate complex would be expected to be weakened relative to the conventional substrates, and provide the most opportunity for intervention of the SH_2 pathway. This possibility merits further experimental investigation.

Both the recent computational studies of Feldgus and Landis, and the experimental contributions of Imamoto and Gridnev, have revived the possibility that the turnover-limiting step in enantioselective hydrogenation is migratory insertion rather than dihydrogen addition. Either fits in with the modified Quadrant Rule. The lack of extensive experimental evidence on dihydride intermediates (the only characterized case being some way towards the alkylhydride state because of an agostic Rh–H–C_α linkage) makes generalization difficult. At the same time, it is abundantly clear that the stereochemical course of very large numbers of rhodium-catalyzed enantioselective hydrogenations are governed by factors that permit accurate predictions based on the geometrical model (see Fig. 31.12). There is a good case for the conclusion that different catalyst/substrate systems operate by the same pathway, and with the same factors controlling enantioselectivity, which is defined at the stage of migratory insertion. The relative heights of energy barriers in the H_2 addition, Rh–H insertion steps will vary from case to case.

Since there are unresolved issues in the fine detail of reaction mechanism, it is worth recalling an earlier publication on reactive intermediates in iridium hydrogenation [61]. In general, conventional Ir diphosphine complexes turnover slowly or not at all when enantioselective hydrogenation of standard substrates is attempted, and essentially all the practical and useful recent synthetic contri-

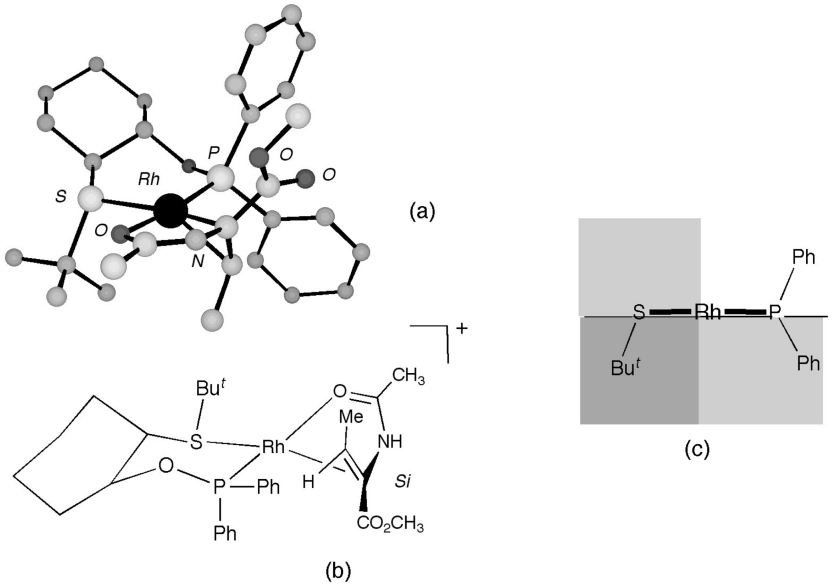

Fig. 31.12 (a) X-ray structure of the enamide complex that corresponds to the "correct" hand of product (from [58]). Solvent hydrogens and counterion are omitted for clarity. (b) Structure of the cation in (a). (c) Application of the Quadrant Rule by these authors.

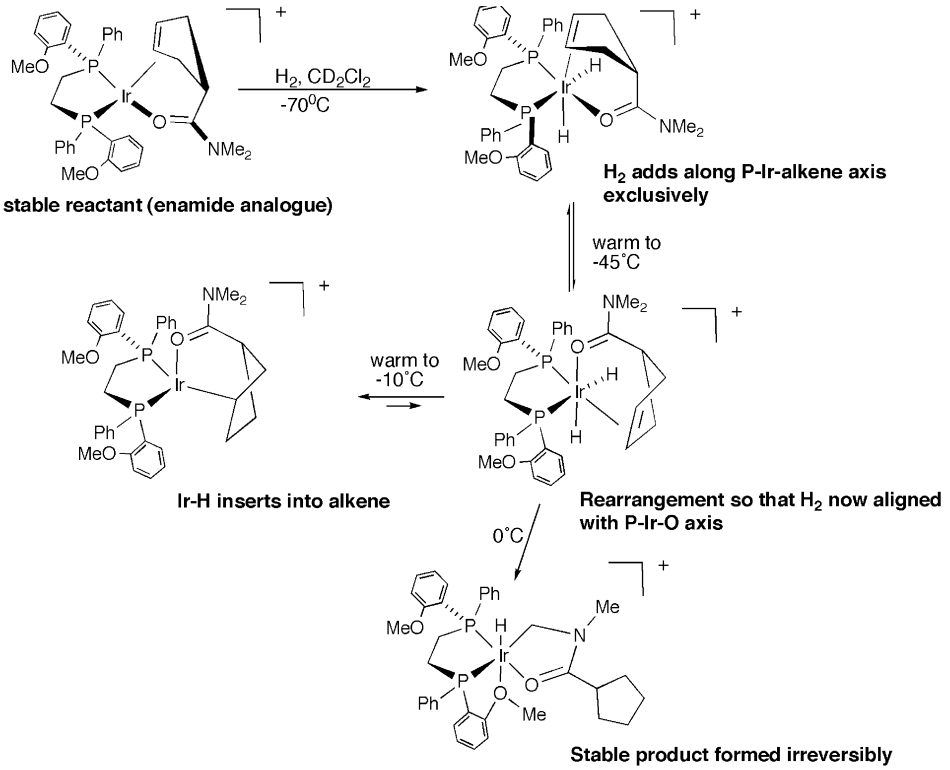

Fig. 31.13 An iridium analogue for the stereochemical course of dihydrogen addition in enantioselective hydrogenation.

butions stem from the use of phosphinamine, phosphinocarbene or aminocarbene chelates. The dihydride intermediates on the P_2Ir^+ reaction pathway are more accessible than in the rhodium case, and reveal features that must surely be relevant to the current debate. Consider the sequence of NMR-characterized species shown in Figure 31.13. The initial addition of dihydrogen to the enamide complex occurs in parallel to the C–Rh–P axis, giving a diastereomeric pair of dihydride complexes that are stable at –70 °C. At higher temperatures complete rearrangement to a pair of H–Rh–O diastereomers occurs, and on further warming thence to an alkylhydride that is stable at ambient temperature. These observations have a clear relevance to the discussion on Rh hydrogenation; they define the likely course of dihydrogen addition and the existence of a low-energy pathway for internal rearrangements of the dihydride intermediate. In terms of the detailed stereochemical pathways defined by Feldgus and Landis, they indicate the strong possibility of easy interconversion mechanisms at each stage, whether or not these pathways have been identified computationally.

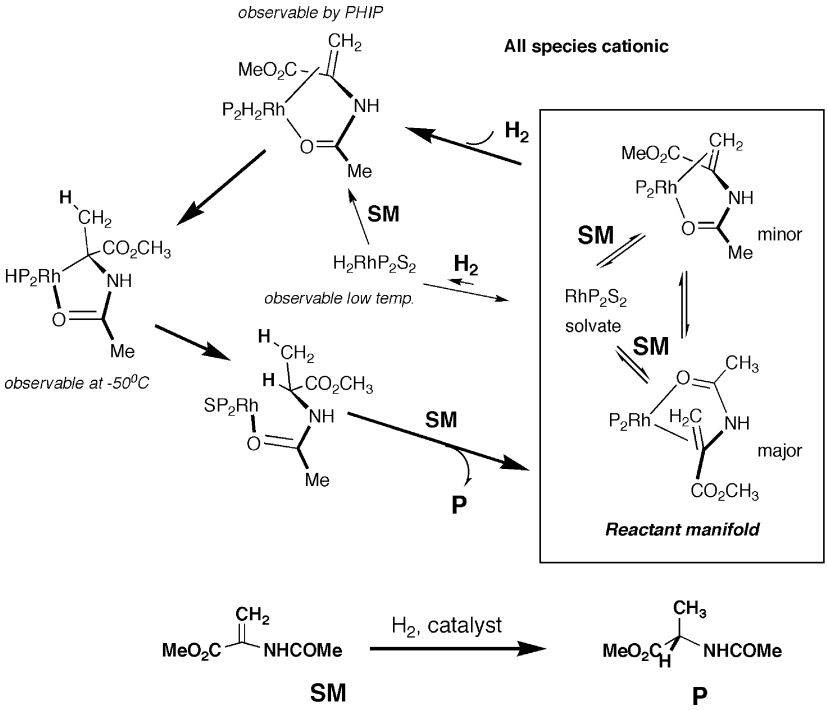

Fig. 31.14 The present state of knowledge on rhodium-complex-catalyzed enantioselective hydrogenation. The H_2 addition stage in the main cycle is predicted to be two-step in DFT calculations; whether that or migratory insertion is turnover-limiting remains debatable.

A summary of the status quo might state that current models can accurately predict the stereochemical sense of dehydroamino acid hydrogenation for a given ligand. There is still some uncertainty over the nature of the turnover-limiting transition state, which could be either H_2 addition or migratory insertion, depending on specific factors for the particular reaction. The predicted stereochemical sense is the same, however, based on analysis of a modified six-coordinate quadrant model arising from the most sterically favorable enamide dihydride. The alternative "hydrogen-first, then alkene" model proposed by Gridnev and Imamoto leads to the same conclusions, but the relative binding constants for hydrogen and dehydroamino acid militate against this pathway in most cases. It could well be important in those examples where the substrate is intrinsically weakly binding, as is found in the hydrogenation of *β*,*β*-disubstituted dehydroamino acids. The state of current knowledge on intermediates in rhodium-complex-catalyzed enantioselective hydrogenation is summarized in Figure 31.14, specifying the route for production of the favored enantiomer [62].

31.3
Ruthenium-Complex-Catalyzed Hydrogenations

Far more ruthenium-complex-catalyzed enantioselective hydrogenation has been directed towards ketone reduction rather than alkene reduction. Recent studies carried out on the mechanism of C=C hydrogenation has been rather limited. One reason for this has been the contrast between the ease of access of the active hydrogenation catalyst in rhodium chemistry and ruthenium chemistry. For rhodium, the cationic complex L_2Rh^+(alkene), where (alkene) is cycloocta-1,5-diene or norbornadiene, is readily and almost universally available; otherwise the active catalyst can be prepared *in situ* directly from the ligand. Generating the catalyst has always been more challenging in ruthenium hydrogenations, and a variety of protocols have been published over the years. Recent publications have provided access to cationic L_2Ru^+HX species where X represents a labile ligand or solvent molecules [63]. The additional hydride compared to the corresponding rhodium species serves to emphasize differences in reaction mechanisms between the two catalyst families.

31.3.1
Reactive Intermediates in Ruthenium-Complex-Catalyzed Hydrogenations

The most successful attempt to capture reactive intermediates stems from the NMR-based studies of Bergens and Wiles [64]. The accessibility of a BINAP Ru–H complex with labile ligands permits the solution characterization of an enamide complex from (*Z*)-*α*-methyl acetamidocinnamate (MAC) with a single solvent molecule in place, *trans*- to the hydride. The configuration of the bound alkene is identical to that of the final hydrogenation product (i.e., the major diastereomer is the precursor of product). On warming from –40 °C to –20 °C, this is converted into a Ru alkyl, itself stable until the addition of dihydrogen, which promotes the formation of the hydrogenated product. The coordination geometry of both intermediates was established by HETCOR and other techniques. Theses experiments provide a simple model for ruthenium-catalyzed hydrogenation of dehydroamino acids, and may be relevant to other bidentate reactants. These investigations are summarized in more detail in [14].

31.3.2
Kinetic Analysis of Ruthenium-Complex-Catalyzed Hydrogenations

There is only one detailed kinetic study of ruthenium enantioselective hydrogenation, in this case involving (BINAP)$Ru(OAc)_2$, and MAC [65]. The extensive study involved reaction kinetics, isotopic analysis of reaction components and products, and *in-situ* NMR. The derived catalytic cycle is shown in Figure 31.15, differing from the Bergens' studies described above in that the intermediates – both observed and assumed – are neutral rather than cationic. Right up to the formation of the alkylruthenium intermediate, the individual steps are revers-

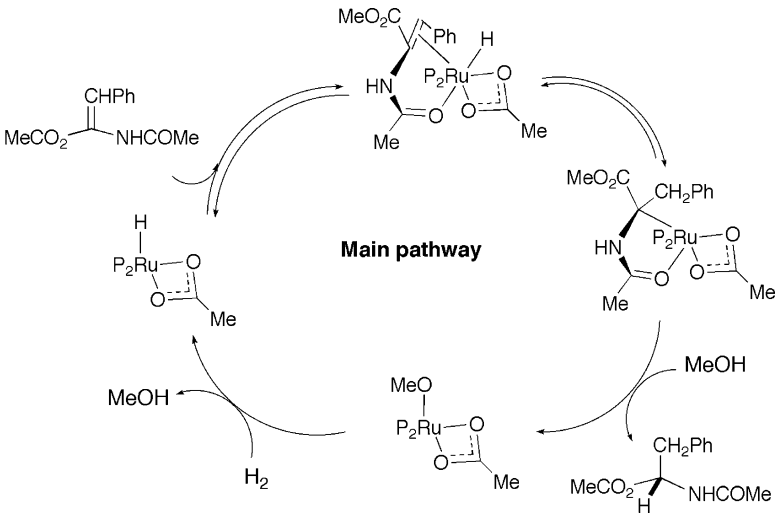

Fig. 31.15 Mechanism of the enantioselective hydrogenation of enamides by Ru BINAP, giving the opposite stereochemical course to the corresponding Rh catalyst. Note the heterolytic nature of the addition process with one of the two hydrogens arising from solvent.

ible. Formally, the second hydrogen comes from the solvent MeOH as well as molecular hydrogen, as had been seen in earlier studies from the same laboratory in α,β-unsaturated acid reductions [66]. In the kinetic studies, a first-order response to both [H_2] and [catalyst] was observed, but a more complex relationship with [substrate] was seen, close to inverse first-order. Individual runs follow first-order kinetics at [H_2] <7 bar, that do not reflect this inhibition by substrate, and this is interpreted to reflect the (irreversible) formation of an enamide-derived inert byproduct P_2RuH(OAc)S (S = substrate), with a geometry that is unfavorable for H-transfer. This supposed byproduct was observed by NMR, under conditions that simulate catalytic hydrogenation at –60 °C. It is the [P_2RuH(OAc)] species that is the true catalyst precursor.

31.4 Iridium-Complex-Catalyzed Hydrogenations

31.4.1 Background

The classical notion has been that iridium complexes can be effective hydrogenation catalysts, with defined limitations. In this respect, Crabtree and Morris made the key breakthroughs [9], and their catalyst (Fig. 31.16) has been widely employed for the reduction of simple alkenes. It was widely successful in the di-

rected (diastereoselective) hydrogenation of alkenes carrying an adjacent polar group [67], but application to enantioselective hydrogenation was lacking. This situation changed with the demonstration by Lightfoot and Pfaltz that chelate P-N-ligated Ir complexes were successful catalysts for enantioselective hydrogenation. The publication has stimulated several parallel developments by other groups as well as improvements in the original Pfaltz ligand, resulting in the present capability to achieve high enantioselectivity in a wide range of cases with readily accessible catalyst systems [68].

31.4.2
Mechanistic and Computational Studies

The mechanistic basis of iridium-complex-catalyzed enantioselective hydrogenation is less secure than in the rhodium case. It is well known that square-planar iridium complexes exhibit a stronger affinity for dihydrogen than their rhodium counterparts. In earlier studies, Crabtree et al. investigated the addition of H_2 to their complex and observed two stereoisomeric intermediate dihydrides in the hydrogenation of the coordinated cycloocta-1,5-diene. The observations were in contrast to the course of H_2 addition to *bis*-phosphine iridium complexes [69].

This formed a basis for the study of the H_2 addition step in a precatalyst for Ir enantioselective hydrogenation [70]. By NMR, it proved possible to characterize a single diastereomer of the initial addition product at –40 °C in THF, the configuration of which was defined by nOe methods. This was converted into a mixture of two diastereomers of the disolvate dihydride with release of cyclooctane at 0 °C. In all cases, H *trans*-N is preferred over H *trans*-P, as was originally observed by Crabtree. The investigations were completed by DFT computational studies on the initial steps of the reaction sequence as a model for the stereose-

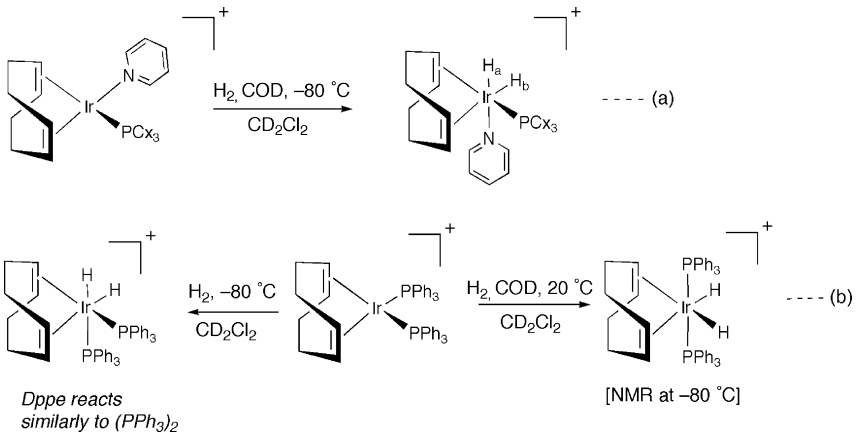

Fig. 31.16 Stable hydrides formed from (a) amine/phosphine iridium cations and (b) *bis*-phosphine or diphosphine iridium cations.

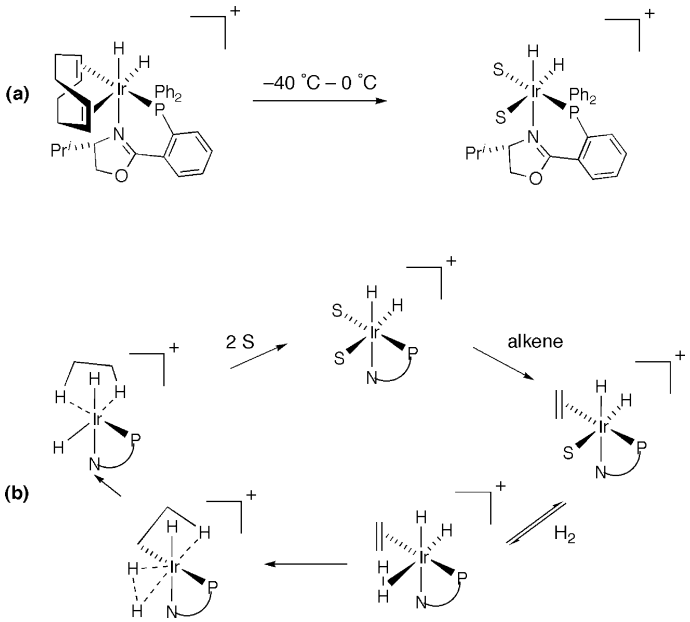

Fig. 31.17 (a) Experimental observation of dihydrides in the PHOXIr$^+$ system by NMR (S=THF). (b) The DFT-derived mechanism for Ir-catalyzed enantioselective hydrogenation involving the sequential addition of two molecules of dihydrogen, with a single H-atom transfer from each one (S=CH_2Cl_2).

lectivity of the initial step in iridium-complex-catalyzed asymmetric hydrogenation. This defines the relative energies of the cycloocta-1,5-diene dihydride diastereomers and the solvate (methanol) dihydride diastereomers. The lowest energy structures at these two levels are shown in Figure 31.17.

An informative set of calculations was carried out by Brandt et al., coupled to experimental studies that demonstrated first-order dependence of the turnover rate on both catalyst and H_2, and zero-order dependence on alkene (*α*-methyl-(*E*)-stilbene) concentration [71]. The incentive for this investigation was the absence of any characterized advanced intermediates on the catalytic pathway. As a result of the computation, a catalytic cycle (for ethene) was proposed in which H_2 addition to iridium was followed by alkene coordination and migratory insertion. The critical difference in this study was the proposal that a second molecule of H_2 is involved that facilitates formation of the Ir alkylhydride intermediate. In addition, the reductive elimination of R–H and re-addition of H_2 are concerted. This postulate was subsequently challenged. For hydrogenation of styrene by the "standard" Pfaltz catalyst, ES-MS analysis of the intermediates formed at different stages in the catalytic cycle revealed only Ir(I) and Ir(III) species, supporting a cycle (at least under low-pressure conditions in the gas

phase) for which a dihydridoalkene complex is assembled and undergoes successive migratory insertion and reductive elimination [72].

31.4.3
Counter-Ion Effects

A remarkable feature of iridium enantioselective hydrogenation is the promotion of the reaction by large non-coordinating anions [73]. This has been the subject of considerable activity (anticipated in an earlier study by Osborn and coworkers) on the effects of the counterion in Rh enantioselective hydrogenation [74]. The iridium chemistry was motivated by initial synthetic limitations. With PF_6^- as counterion to the ligated Ir cation, the reaction ceases after a limited number of turnovers because of catalyst deactivation. The mechanism of

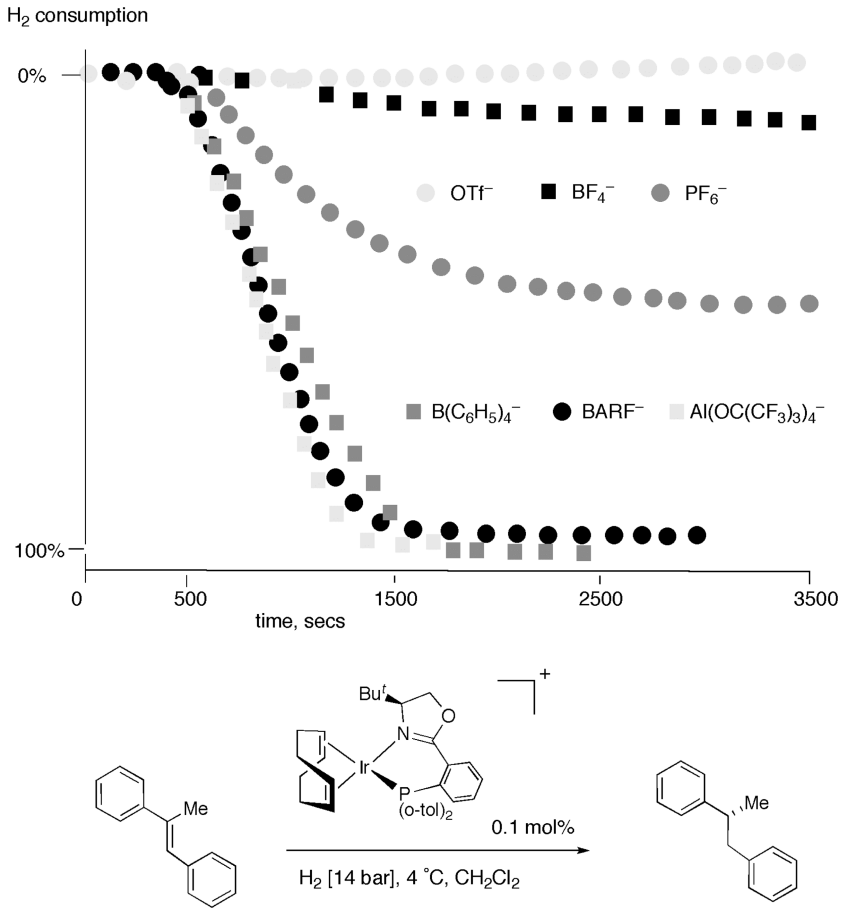

Fig. 31.18 Anion effects on the enantioselective hydrogenation shown (adapted from [77]).

deactivation is similar to that originally observed with Crabtree's catalyst, in that an inactive dimeric trihydride is formed irreversibly [75]. When the large anion BARf is employed, the reaction is considerably faster, and not subject to inhibition. This observation stimulated a body of physico-chemical studies on the nature of ion-pair effects in these and related complexes [76]. In a detailed kinetic study of hydrogenation, the large effect of counter-ion on reaction rate was not reflected in any influence on the *ee* of the reaction, which was the same (within experimental error) for a series of three bulky and three small anions (Fig. 31.18). In the course of these studies it was found that: (i) CH_2Cl_2 is the best solvent; (ii) the catalytic reaction is inhibited by water at very low concentrations, and success therefore requires careful drying of the reaction components; (iii) there is a first-order dependence on $[H_2]$, and on [catalyst] at low loading; and (iv) the reaction rate decreased slightly with increasing [alkene], but only when the bulky non-coordinating anions were employed [77].

In recent studies, Burgess and coworkers noted that examples of the enantioselective hydrogenation of conjugated dienes are fairly sparse in the literature [78]. They demonstrated that the diene binds strongly to their iminocarbene Ir^+ catalyst under hydrogenation conditions, and the course of reaction changed when the reactant was consumed. This was subsequently controlled by the superior rate of hydrogenation of the monoene enantiomer that is stereochemically the better matched to the configuration of the catalyst. The overall reaction was biphasic, with hydrogenation of the coordinated diene dominant until it was consumed.

31.5 Summary and Conclusions

Since the first demonstration of enantioselective hydrogenation by Knowles and colleagues at Monsanto, and the important early contributions of Kagan, enantioselective hydrogenation has consistently been central to the development of enantioselective catalysis. The present chapter concentrates on the hydrogenation of alkenes, though since the mid-1980s the hydrogenation of ketones has been pursued with equal vigor. Part of the reason for this is the sheer simplicity of the procedure, and the versatility of the outcome. Equally, the ability to carry out enantioselective hydrogenation on an industrial scale has provided a strong impetus for catalyst discovery and development, with several important recent developments having arisen from industrial laboratories. The first wave of development exclusively involved rhodium catalysts, and these dominated up to 1985. However, with the advent of ruthenium BINAP catalysts, introduced by Noyori and Takaya, the emphasis changed dramatically. The increased versatility and the productive involvement of both C=C and C=O functionalities made this the focal point of enantioselective hydrogenation for a decade, and led to the award of the Nobel Prize (of course equally shared with Sharpless for enantioselective oxidation) jointly to Knowles and Noyori. The recent upsurge of interest

has had several drivers. A new generation of ligands has increased the scope of the rhodium-complex-catalyzed reaction and further improved enantioselectivity. The discovery and development of iridium enantioselective hydrogenation by Pfaltz and coworkers has extended the substrate scope. The reintroduction of monophosphine catalysts for enantioselective hydrogenation, and especially the recognition that two different phosphine ligands (only one need be chiral) can operate cooperatively, offers exciting new prospects. As the synthetic utility is extended, it is equally necessary to address the mechanistic aspects and to provide a complete picture of this centrally important reaction.

Acknowledgments

The author thanks Dr. Monika Mayr, Dr. Linnea Soler and Jeremy Taylor for their helpful comments made on the draft of this chapter.

Abbreviations

AE	absorption-emission
DFT	density function theory
ES-MS	electrospray-mass spectrometry
MAC	(*Z*)-*α*-methyl acetamidocinnamate
MM	molecular mechanics
UFF	universal force field

References

1 Osborn, J. A., Jardine, F. H., Young, G. W., Wilkinson, G., *J. Chem. Soc. A*, **1966**, 1711.

2 Horner, L., Winkler, H., *Annalen*, **1965**, *685*, 1; Horner, L., Balzer, W. D., Peterson, D. J., *Tetrahedron Lett.*, **1966**, 3315; Korpiun, O., Mislow, K., *J. Am. Chem. Soc.*, **1967**, *89*, 4784; Korpiun, O., Lewis, R. A., Chickos, J., Mislow, K., *J. Am. Chem. Soc.*, **1968**, *90*, 4842; Naumann, K., Zon, G., Mislow, K., *J. Am. Chem. Soc.*, **1969**, *91*, 7012.

3 Horner, L., Siegel, H., Buethe, H., *Angew. Chem., Int. Ed.*, **1968**, *7*, 942.

4 Knowles, W. S., Sabacky, M. J., *Chem. Commun.*, **1968**, 1445.

5 Kagan, H. B., Dang, T. P., *J. Am. Chem. Soc.*, **1972**, *94*, 6429.

6 Vineyard, B. D., Knowles, W. S., Sabacky, M. J., Bachman, G. L., Weinkauff, D. J., *J. Am. Chem. Soc.*, **1977**, *99*, 5946.

7 Chaloner, P. A., Esteruelas, M. A., Joo, F., Oro, L. A., *Homogeneous Hydrogenation*, Kluwer, Dordrecht, **1994**; Noyori, R., *Asymmetric Catalysis in Organic Synthesis* (especially Chapter 2), John Wiley & Sons, Inc., New York, **1994**; Ojima, I. (Ed.), *Catalytic Asymmetric Synthesis*, John Wiley & Sons, Inc., New York, **2000**.

8 Hallman, P. S., Evans, D., Osborn, J. A., Wilkinson, G., *Chem. Commun.*, **1967**, 305; Hallman, P. S., McGarvey, B. R., Wilkinson, G., *J. Chem. Soc. A*, **1968**, 3143; Rose, D., Gilbert, J. D., Richardson, R. P., Wilkinson, G., *J. Chem. Soc. A*, **1969**, 2610.

9 Crabtree, R.H., Felkin, H., Morris, G.E., *Chem. Commun.*, **1976**, 716; Crabtree, R.H., Felkin, H., Morris, G.E., *J. Organomet. Chem.*, **1977**, *141*, 205.

10 Noyori, R., Ohta, M., Hsiao, Y., Kitamura, M., Ohta, T., Takaya, H., *J. Am. Chem. Soc.*, **1986**, *108*, 7117; Takaya, H., Ohta, T., Sayo, N., Kumobayashi, H., Akutagawa, S., Inoue, S., Kasahara, I., Noyori, R., *J. Am. Chem. Soc.*, **1987**, *109*, 1596; Ohta, T., Takaya, H., Kitamura, M., Nagai, K., Noyori, R., *J. Org. Chem.*, **1987**, *52*, 3174.

11 Kitamura, M., Ohkuma, T., Inoue, S., Sayo, N., Kumobayashi, H., Akutagawa, S., Ohta, T., Takaya, H., Noyori, R., *J. Am. Chem. Soc.*, **1988**, *110*, 629; Noyori, R., Ohkuma, T., Kitamura, M., Takaya, H., Sayo, N., Kumobayashi, H., Akutagawa, S., *J. Am. Chem. Soc.*, **1987**, *109*, 5856.

12 Lightfoot, A., Schnider, P., Pfaltz, A., *Angew. Chem., Int. Ed.*, **1998**, *37*, 2897.

13 Blaser, H.-U., Schmidt, E. (Eds.), *Asymmetric Catalysis on an Industrial Scale; Challenges, Approaches and Solutions*. Wiley-VCH, New York, **2004**.

14 Brown, J.M., in: Jacobsen, E.N., Pfaltz, A., Yamamoto, H. (Eds.), *Comprehensive Asymmetric Catalysis*, Volume I, Chapter 5.1. Springer, Berlin, **1999**, pp. 121.

15 (a) Landis, C.R., Halpern, J., *J. Am. Chem. Soc.*, **1987**, *109*, 1746; (b) Halpern, J., *Science*, **1982**, *217*, 401; (c) Halpern, J., Chan, A.S.C., *J. Am. Chem. Soc.*, **1980**, *102*, 838; (d) Chan, A.S.C., Pluth, J.J., Halpern, J., *J. Am. Chem. Soc.*, **1980**, *102*, 5952; (e) Sun, Y.K., Landau, R.N., Wang, J., Leblond, C., Blackmond, D.G., *J. Am. Chem. Soc.*, **1996**, *118*, 1348.

16 Brown, J.M., Chaloner, P.A., Nicholson, P.N., *J. Chem. Soc., Chem. Commun.*, **1978**, 646; Brown, J.M., Chaloner, P.A., *Tetrahedron Lett.*, **1978**, 1877; Brown, J.M., Chaloner, P.A., *J. Chem. Soc., Chem. Commun.*, **1978**, 321; Brown, J.M., Chaloner, P.A., Descotes, G., Glaser, R., Lafont, D., Sinou, D., *J. Chem. Soc., Chem. Commun.*, **1979**, 611; Brown, J.M., Chaloner, P.A., *J. Chem. Soc., Chem. Commun.*, **1979**, 613; Brown, J.M., Chaloner, P.A., *J. Chem. Soc., Chem. Commun.*, **1980**, 344; Brown, J.M., Chaloner, P.A., Glaser, R., Geresh, S., *Tetrahedron*, **1980**, *36*, 815; Descotes, G., Lafont, D., Sinou, D., Brown, J.M., Chaloner, P.A., Parker, D., *New J. Chem.*, **1981**, *5*, 167.

17 Drexler, H.-J., Baumann, W., Spannenberg, A., Fischer, C., Heller, D., *J. Organometal. Chem.*, **2001**, *621*, 89; Borner, A., Heller, D., *Tetrahedron Lett.*, **2001**, *42*, 223; Braun, W., Salzer, A., Drexler, H.-J., Spannenberg, A., Heller, D., *Dalton Trans.* **2003**, 1606.

18 Brown, J.M., Canning, L.R., Downs, A.J., Forster, A.M., *J. Organomet. Chem.*, **1983**, *255*, 103.

19 Brown, J.M., Chaloner, P.A., Parker, D., *Adv. Chem. Ser.*, **1982**, *196*, 355.

20 Brown, J.M., Chaloner, P.A., Morris, G.A., *J. Chem. Soc. Chem. Commun.*, **1983**, 664; Brown, J.M., Chaloner, P.A., Morris, G.A., *J. Chem. Soc. Perkin Trans. 2*, **1987**, 1583; Ramsden, J.A., Claridge, T.D.W., Brown, J.M., *J. Chem. Soc. Chem. Commun.*, **1995**, 2469.

21 Burk, M.J., Feaster, J.E., Nugent, W.A., Harlow, R.L., *J. Am. Chem. Soc.*, **1993**, *115*, 10125.

22 Muci, A.R., Campos, K.R., Evans, D.A., *J. Am. Chem. Soc.*, **1995**, *117*, 9075.

23 Imamoto, T., Watanabe, J., Wada, Y., Masuda, H., Yamada, H., Tsuruta, H., Matsukawa, S., Yamaguchi, K., *J. Am. Chem. Soc.*, **1998**, *120*, 1635; Miura, T., Imamoto, T., *Tetrahedron Lett.*, **1999**, *40*, 4833; Gridnev, I.D., Yamanoi, Y., Higashi, N., Tsuruta, H., Yasutake, M., Imamoto, T., *Adv. Synth. Catal.*, **2001**, *343*, 118; Gridnev, I.D., Yasutake, M., Higashi, N., Imamoto, T., *J. Am. Chem. Soc.*, **2001**, *123*, 5268; Imamoto, T., *Pure Appl. Chem.*, **2001**, *73*, 373; Ohashi, A., Imamoto, T., *Tetrahedron Lett.*, **2001**, *42*, 1099; Yasutake, M., Gridnev, I.D., Higashi, N., Imamoto, T., *Org. Lett.*, **2001**, *3*, 1701; Ohashi, A., Kikuchi, S., Yasutake, M., Imamoto, T., *Eur. J. Org. Chem.*, **2002**, 2535; Crepy, K.V.L., Imamoto, T., *Adv. Synth. Catal.*, **2003**, *345*, 79; Oohara, N., Katagiri, K., Imamoto, T., *Tetrahedron: Asymmetry*, **2003**, *14*, 2171.

24 Pye, P.J., Rossen, K., Reamer, R.A., Tsou, N.N., Volante, R.P., Reider, P.J., *J. Am. Chem. Soc.*, **1997**, *119*, 6207; Ros-

sen, K., Pye, P.J., DiMichele, L.M., Volante, R.P., Reider, P.J., *Tetrahedron Lett.*, **1998**, *39*, 6823.
25 Tang, W.J., Zhang, X.M., *Chem. Rev.*, **2003**, *103*, 3029.
26 Claver, C., Fernandez, E., Gillon, A., Heslop, K., Hyett, D.J., Martorell, A., Orpen, A.G., Pringle, P.G., *Chem. Commun.*, **2000**, 961; Reetz, M.T., Sell, T., *Tetrahedron Lett.*, **2000**, *41*, 6333; van den Berg, M., Minnaard, A.J., Schudde, E.P., van Esch, J., de Vries, A.H.M., de Vries, J.G., Feringa, B.L., *J. Am. Chem. Soc.*, **2000**, *122*, 11539; van den Berg, M., Haak, R.M., Minnaard, A.J., De Vries, A.H.M., De Vries, J.G., Feringa, B.L., *Adv. Synth. Catal.*, **2002**, *344*, 1003.
27 Gridnev, I.D., Higashi, N., Asakura, K., Imamoto, T., *J. Am. Chem. Soc.*, **2000**, *122*, 7183.
28 Gridnev, I.D., Higashi, N., Imamoto, T., *Organometallics*, **2001**, *20*, 4542.
29 Gridnev, I.D., Yamanoi, Y., Higashi, N., Tsuruta, H., Yasutake, M., Imamoto, T., *Adv. Synth. Catal.*, **2001**, *343*, 118; Gridnev, I.D., Imamoto, T., *Organometallics*, **2001**, *20*, 545.
30 Heinrich, H., Giernoth, R., Bargon, J., Brown, J.M., *Chem. Commun.*, **2001**, 1296.
31 Halpern, J., Wong, C.S., *J. Chem. Soc., Chem. Commun.*, **1973**, 629.
32 Brown, J.M., Parker, D., *Organometallics*, **1982**, *1*, 950.
33 Burk, M.J., Casy, G., Johnson, N.B., *J. Org. Chem.*, **1998**, *63*, 6084.
34 Gridnev, I.D., Higashi, N., Imamoto, T., *J. Am. Chem. Soc.*, **2000**, *122*, 10486.
35 Feldgus, S., Landis, C.R., *Organometallics*, **2001**, *20*, 2374.
36 Harthun, A., Kadyrov, R., Selke, R., Bargon, J., *Angew. Chem., Int. Ed. Engl.*, **1997**, *36*, 1103.
37 Giernoth, R., Heinrich, H., Adams, N.J., Deeth, R.J., Bargon, J., Brown, J.M., *J. Am. Chem. Soc.*, **2000**, *122*, 12381.
38 Samuel, O., Couffignal, R., Lauer, M., Zhang, S.Y., Kagan, H.B., *Nouv. J. Chim.*, **1981**, *5*, 15, see also: Fryzuk, M.D., Bosnich, B., *J. Am. Chem. Soc.*, **1977**, *99*, 6262; Pavlov, V.A., Klabunovskii, E.I., Struchkov, Y.T., Voloboev, A.A., Yanovsky, A.I., *J. Mol. Catal.*, **1988**, *44*, 217.
39 Kyba, E.P., Davis, R.E., Juri, P.N., Shirley, K.R., *Inorg. Chem.* **1981**, *20*, 3616.
40 Knowles, W.S., *Accounts Chem. Res.*, **1983**, *16*, 106.
41 Marinetti, A., Jus, S., Genet, J.P., *Tetrahedron Lett.*, **1999**, *40*, 8365.
42 Gridnev, I.D., Imamoto, T., *Accounts Chem. Res.*, **2004**, *37*, 633.
43 Drexler, H.J., Zhang, S.L., Sun, A.L., Spannenberg, A., Arrieta, A., Preetz, A., Heller, D., *Tetrahedron: Asymmetry*, **2004**, *15*, 2139.
44 Landis, C.R., Hilfenhaus, P., Feldgus, S., *J. Am. Chem. Soc.*, **1999**, *121*, 8741.
45 Feldgus, S., Landis, C.R., *J. Am. Chem. Soc.*, **2000**, *122*, 12714.
46 Ramsden, J.A., Claridge, T., Brown, J.M., *J. Chem. Soc. Chem. Commun.*, **1995**, 2469, and references therein.
47 Li, M., Tang, D., Luo, X., Shen, W., *Int. J. Quantum Chem.*, **2005**, *102*, 53.
48 Knowles, W.S., Sabacky, M.J., Vineyard, B.D., *J. Chem. Soc. Chem. Commun.*, **1972**, 10.
49 Guillen, F., Fiaud, J.-C., *Tetrahedron Lett.*, **1999**, *40*, 2939; Guillen, F., Rivard, M., Toffano, M., Legros, J.-Y., Daran, J.-C., *Tetrahedron*, **2002**, *58*, 5895; Fiaud, J.-C., Dobrota, C., Toffano, M., Fiaud, J.-C., *Tetrahedron Lett.*, **2004**, *45*, 8153.
50 Bernsmann, H., van den Berg, M., Hoen, R., Minnaard, A.J., Mehler, G., Reetz, M.T., De Vries, J.G., Feringa, B.L., *J. Org. Chem.*, **2005**, *70*, 943.
51 Hoen, R., van den Berg, M., Bernsmann, H., Minnaard, A.J., de Vries, J.G., Feringa, B.L., *Org. Lett.*, **2004**, *6*, 1433, and references therein.
52 van den Berg, M., et al., *Adv. Synth. Catal.*, **2003**, *345*, 308.
53 Reetz, M.T., Mehler, G., *Tetrahedron Lett.*, **2003**, *44*, 4593; Reetz, M.T., Mehler, G., Melswinkel, A., Sell, T., *Tetrahedron: Asymmetry*, **2004**, *15*, 3483; Reetz, M.T., Li, X., *Angew. Chem., Int. Ed.*, **2005**, *44*, 2959.
54 Wu, H.P., Hoge, G., *Org. Lett.*, **2004**, *6*, 3645; Reetz, M.T., Li, X.G., *Tetrahedron*, **2004**, *60*, 9709; Jerphagnon, T., Renaud, J.L., Demonchaux, P., Ferreira, A., Bruneau, C., *Adv. Synth. Catal.*, **2004**, *346*, 33;

Huang, H.M., Liu, X.C., Chen, S., Chen, H.L., Zheng, Z., *Tetrahedron: Asymmetry*, **2004**, *15*, 2011; Hsiao, Y., et al., *J. Am. Chem. Soc.*, **2004**, *126*, 9918; Hoge, G., Samas, B., *Tetrahedron: Asymmetry*, **2004**, *15*, 2155; Tang, W., Wu, S., Zhang, X., *J. Am. Chem. Soc.*, **2003**, *125*, 9570; Tang, W., Wang, W., Chi, Y., Zhang, X., *Angew. Chem.-Int. Ed.*, **2003**, *42*, 3509; Tang, W., Zhang, X., *Org. Lett.*, **2002**, *4*, 4159; Pena, D., Minnaard, A.J., de Vries, J.G., Feringa, B.L., *J. Am. Chem. Soc.*, **2002**, *124*, 14552; Yasutake, M., Gridnev, I.D., Higashi, N., Imamoto, T., *Org. Lett.*, **2001**, *3*, 1701; Zhu, G., Chen, Z., Zhang, X., *J. Org. Chem.*, **1999**, *64*, 6907; Zhu, G., Casalnuovo, A.L., Zhang, X., *J. Org. Chem.*, **1998**, *63*, 8100.

55 Heller, D., Holz, J., Komarov, I., Drexler, H.-J., You, J., Drauz, K., Borner, A., *Tetrahedron: Asymmetry*, **2002**, *13*, 2735; Heller, D., Drexler, H.-J., You, J., Baumann, W., Drauz, K., Krimmer, H.-P., Borner, A., *Chem. Eur. J.*, **2002**, *8*, 5196.

56 Drexler, H.-J., Baumann, W., Schmidt, T., Zhang, S., Sun, A., Spannenberg, A., Fischer, C., Buschmann, H., Heller, D., *Angew. Chem., Int. Ed.*, **2005**, *44*, 1184.

57 Yasutake, M., Gridnev, I.D., Higashi, N., Imamoto, T., *Org. Lett.*, **2001**, *3*, 1701.

58 Evans, D.A., Michael, F.E., Tedrow, J.S., Campos, K.R., *J. Am. Chem. Soc.*, **2003**, *125*, 3534.

59 Drexler, H.J., You, J.S., Zhang, S.L., Fischer, C., Baumann, W., Spannenberg, A., Heller, D., *Org. Process Res. Dev.*, **2003**, *7*, 355.

60 Tang, W.J., Wu, S.L., Zhang, X.M., *J. Am. Chem. Soc.*, **2003**, *125*, 9570.

61 Brown, J.M., Maddox, P.J., *Chem. Commun.*, **1987**, 1278.

62 Brown, J.M., *J. Organomet. Chem.*, **2004**, *689*, 4006.

63 Wiles, J.A., Bergens, S.H., Vanhessche, K.P.M., Dobbs, D.A., Rautenstrauch, V., *Angew. Chem.-Int. Ed.*, **2001**, *40*, 914; Wiles, J.A., Daley, C.J.A., Hamilton, R.J., Leong, C.G., Bergens, S.H., *Organometallics*, **2004**, *23*, 4564.

64 Wiles, J.A., Bergens, S.H., *Organometallics*, **1999**, *18*, 3709; Wiles, J.A., Bergens, S.H., *Organometallics*, **1998**, *17*, 2228; Wiles, J.A., Bergens, S.H., Young, V.G., *J. Am. Chem. Soc.*, **1997**, *119*, 2940.

65 Kitamura, M., Tsukamoto, M., Bessho, Y., Yoshimura, M., Kobs, U., Widhalm, M., Noyori, R., *J. Am. Chem. Soc.*, **2002**, *124*, 6649.

66 Ohta, T., Takaya, H., Noyori, R., *Tetrahedron Lett.*, **1990**, *31*, 7189.

67 Crabtree, R.H., Davis, M.W., *Organometallics*, **1983**, *2*, 681; Crabtree, R.H., Davis, M.W., *J. Org. Chem.*, **1986**, *51*, 2655.

68 Examples include: Kaellstroem, K., Hedberg, C., Brandt, P., Bayer, A., Andersson, P.G., *J. Am. Chem. Soc.*, **2004**, *126*, 14308; Trifonova, A., Diesen, J.S., Chapman, C.J., Andersson, P.G., *Org. Lett.*, **2004**, *6*, 3825; Smidt, S.P., Menges, F., Pfaltz, A., *Org. Lett.*, **2004**, *6*, 2023; Liu, D., Tang, W., Zhang, X., *Org. Lett.*, **2004**, *6*, 513; Schenkel, L.B., Ellman, J.A., *J. Org. Chem.*, **2004**, *69*, 1800–1802; Drury, W.J., Zimmermann, N., Keenan, M., Hayashi, M., Kaiser, S., Goddard, R., Pfaltz, A., *Angew. Chem.-Int. Ed.*, **2004**, *43*, 70; Mazet, C., Smidt, S.P., Meuwly, M., Pfaltz, A., *J. Am. Chem. Soc.*, **2004**, *126*, 14176; Perry, M.C., Cui, X.H., Powell, M.T., Hou, D.R., Reibenspies, J.H., Burgess, K., *J. Am. Chem. Soc.*, **2003**, *125*, 113; Menges, F., Pfaltz, A., *Adv. Synth. Catal.*, **2002**, *344*, 40–44; Cozzi, P.G., Zimmermann, N., Hilgraf, R., Schaffner, S., Pfaltz, A., *Adv. Synth. Catal.*, **2001**, *343*, 450; Blankenstein, J., Pfaltz, A., *Angew. Chem.-Int. Ed.*, **2001**, *40*, 4445.

69 Crabtree, R.H., Felkin, H., Morris, G.E., *J. Organomet. Chem.*, **1977**, *141*, 205; Crabtree, R.H., Felkin, H., Khan, T., Morris, G.E., *J. Organomet. Chem.*, **1978**, *144*, C15; Crabtree, R.H., Felkin, H., Fillebeen-Khan, T., Morris, G.E., *J. Organomet. Chem.*, **1979**, *168*, 183.

70 Mazet, C., Smidt, S.P., Meuwly, M., Pfaltz, A., *J. Am. Chem. Soc.*, **2004**, *126*, 14176.

71 Brandt, P., Hedberg, C., Andersson, P.G., *Chem.-Eur. J.*, **2003**, *9*, 339.

72 Dietiker, R., Chen, P., *Angew. Chem., Int. Ed.*, **2004**, *43*, 5513.

73 Blackmond, D.G., Lightfoot, A., Pfaltz, A., Rosner, T., Schnider, P., Zimmerman, N., *Chirality*, **2000**, *12*, 442.

74 Buriak, J.M., Klein, J.C., Herrington, D.G., Osborn, J.A., *Chem. Eur. J.*, **2000**, *6*, 139.

75 Smidt, S.P., Pfaltz, A., Martinez-Viviente, E., Pregosin, P.S., Albinati, A., *Organometallics*, **2003**, *22*, 1000.

76 Macchioni, A., *Eur. J. Inorg. Chem.*, **2003**, 195; Macchioni, A., *Chem. Rev.*, **2005**, *105*, 2039; Drago, D., Pregosin, P.S., Pfaltz, A., *Chem. Commun.*, **2002**, 286; Martinez-Viviente, E., Pregosin, P.S., *Inorg. Chem.*, **2003**, *42*, 2209; Martinez-Viviente, E., Pregosin, P.S., Vial, L., Herse, C., Lacour, J., *Chem. Eur. J.*, **2004**, *10*, 2912; Pregosin, P.S., Martinez-Viviente, E., Kumar, P.G.A., *J. Chem. Soc. Dalton Trans.*, **2003**, 4007.

77 Smidt, S.P., Zimmermann, N., Studer, M., Pfaltz, A., *Chem.-Eur. J.*, **2004**, *10*, 4685.

78 Cui, X., Ogle, J.W., Burgess, K., *Chem. Commun.*, **2005**, 672; Cui, X., Burgess, K., *J. Am. Chem. Soc.*, **2003**, *125*, 14212.